

**CASTLEBANNY WIND FARM: COLLISION  
RISK MODEL**

**Tom Gittings BSc, PhD, MCIEEM  
Ecological Consultant  
3 Coastguard Cottages  
Roches Point  
Whitegate  
CO. CORK  
[www.gittings.ie](http://www.gittings.ie)**

**REPORT NUMBER: 1623-F4  
STATUS OF REPORT: Revision 3  
DATE OF REPORT: 15 December 2020**

## CONTENTS

	Page
<b>SUMMARY .....</b>	<b>2</b>
<b>1. INTRODUCTION.....</b>	<b>3</b>
<b>2. STATEMENT OF COMPETENCE .....</b>	<b>3</b>
<b>3. DATA SOURCES .....</b>	<b>3</b>
<b>4. METHODOLOGY.....</b>	<b>4</b>
4.1. General approach.....	4
4.2. Data management.....	4
4.3. Review of the vantage point survey coverage and results .....	4
4.4. Collision risk modelling methodology .....	4
<b>5. COLLISION RISK MODEL STAGE 1: BIRD TRANSITS.....</b>	<b>4</b>
5.1. Methodology .....	4
5.1.1. General approach.....	4
5.1.2. Model types .....	5
5.1.3. Viewshed analyses.....	5
5.1.4. Height bands.....	8
5.1.5. Vantage point survey effort .....	9
5.1.6. Parameter values .....	9
5.1.7. Definition of seasonal periods of occurrence .....	9
5.1.8. Diel variation in flight activity.....	10
5.2. Modelling methodology and results.....	10
5.2.1. General models .....	10
5.2.2. Lesser Black-backed Gull stage 1 model.....	13
5.2.3. Hovering Kestrel stage 1 model .....	14
<b>6. COLLISION RISK MODEL STAGE 2: COLLISION PROBABILITY .....</b>	<b>14</b>
6.1. Methodology .....	14
6.2. Results .....	15
<b>7. COLLISION RISK MODEL STAGE 3: COLLISION PREDICTION.....</b>	<b>16</b>
<b>8. CONCLUSIONS.....</b>	<b>18</b>
<b>REFERENCES .....</b>	<b>19</b>
<b>APPENDIX 1      PARAMETER VALUES USED IN THE COLLISION RISK MODELLING</b>	<b>20</b>
<b>LIST OF FIGURES</b>	
Figure 5.1. Relationship between density of flightlines at potential collision height and distance from vantage point location, using data from all species across all vantage points, weighted by total number of flightlines at potential collision height recorded at each vantage point. ....	7
<b>LIST OF MAPS</b>	
Map 1. Wind Farm site and layout. ....	28
Map 2. Vantage point locations and viewsheds included in the collision risk model. ....	29
Map 3. Lesser Black-backed Gull flight activity classification for the Lesser Black-backed Gull Stage 1 model.....	30

## SUMMARY

This report presents the results of collision risk modelling for the proposed Castlebanny Wind Farm, Co. Kilkenny. Basic models were used to generate predicted transits for species with low levels of recorded flight activity. Models incorporating spatial structure were used to generate predicted transits for the more regularly occurring species. The hovering component of the Kestrel flight activity was modelled separately.

The only species with non-negligible collision risks were Sparrowhawk, Buzzard, Curlew, Lesser Black-backed Gull and Sparrowhawk. For Curlew, this may have been an artefact of a procedure used in the preparation of the dataset. For the other species, this reflects the occurrence of resident populations, or regular commuting routes, within, or across, the wind farm site. The significance of the predicted collision risks are assessed in the Ornithology chapter of the *Castlebanny Wind Farm Environmental Assessment Report*.

## 1. INTRODUCTION

This report presents the results of collision risk modelling for the proposed Castlebanny Wind Farm, Co. Kilkenny. The proposed wind farm will comprise 21 turbines. The proposed site layout is shown in Map 1. The turbine model used for the purpose of this collision risk model is a Siemens Gamesa SG 155 wind turbine with a hub height of 107.5 m and a rotor diameter of 155 m, which creates a potential collision height airspace of 30-185 m.

Collision risk modelling uses statistical modelling techniques to predict the likely collision risk. It uses flight activity data from before the construction of a wind farm to calculate the likely risk of birds colliding with turbines in the operational wind farm. There are three stages to the collision risk model. In stage 1, the flight activity data that was recorded is scaled up to represent the overall level of flight activity in the wind farm site across the relevant period (e.g., a full year for a resident species, or a summer or winter for a migrant species). The number of predicted transits of the rotor swept volume in the wind farm is then calculated based on the proportion of the total air space that is occupied by the rotor swept volume. However, most transits of the rotor swept volume will not result in a collision, because for the duration of a transit, most of the rotor swept volume is not occupied by the turbine blades. Therefore, stage 2 of the collision risk model involves calculating the probability that a bird will collide with a turbine blade when it transits the rotor swept volume. Most birds try to avoid the turbine blades, either by avoiding the wind farm area altogether, or by taking evasive action if they are likely to collide with a blade while transiting the wind farm, so it is also necessary to factor in an avoidance rate. This is done in the final stage, where the predicted number of transits are converted to predicted number of collisions by multiplying by the collision probability (assuming no avoidance behaviour) and then correcting for the avoidance rate.

## 2. STATEMENT OF COMPETENCE

Tom Gittings has a BSc in Ecology, a PhD in Zoology and is a member of the Chartered Institute of Ecology and Environmental Management. He has 25 years' experience in professional ecological consultancy work and research. He has specific expertise in ornithological assessments for wind energy projects and has been involved in 29 wind energy projects. His input to these projects has variously included field surveys (including vantage point surveys, breeding wader and raptor surveys and wintering waterbird surveys), collision risk modelling, writing the ornithological sections of EIS/EIAR and NIS reports, expert witness services at oral hearings, and provision of scoping advice and peer review services.

## 3. DATA SOURCES

Two independent vantage point surveys covering the Castlebanny Wind Farm site were carried out. The GNM vantage point survey was carried out across four consecutive seasons between winter 2016/17 and summer 2018 (Gittings, 2020b), while the MWP vantage point survey was carried out across four consecutive seasons between winter 2017/18 and summer 2019 (MWP, 2019a, 2019b, 2019c, 2020). This collision risk model is based on the GNM vantage point survey. Full details about this vantage point survey are provided in the *Castlebanny Wind Farm, Co. Kilkenny: Ornithological Desk Review and Survey Report* (Gittings, 2020b). For various reasons, it was not possible to add the MWP vantage point survey dataset to the dataset used for this collision risk model, or to carry out a comparable stand-alone collision risk model analysis using the MWP vantage point survey dataset.

The MWP vantage point survey data is used in this collision risk model for a comparative analysis of detectability rates (Section 5.1.3). In addition, comparative analyses of sighting rates between the two vantage point surveys are included in the Ornithology chapter of the *Castlebanny Wind Farm Environmental Assessment Report*. These show that there were not any significant differences between the flight activity levels recorded by the two sets of vantage point surveys, so inclusion of the MWP vantage point survey data would not be expected to significantly change the predicted collision risks.

Vector mapping of the proposed turbine locations, and technical specifications for the proposed turbines were provided by Coillte.

## **4. METHODOLOGY**

### **4.1. GENERAL APPROACH**

The collision risk modelling methodology was based on the SNH guidance on collision risk modelling (SNH, 2000), and current practice in collision risk modelling. It also incorporated development of more detailed structured models for species with high levels of potential collision risk, and a separate model of the hovering component of the Kestrel flight activity.

### **4.2. DATA MANAGEMENT**

Before beginning the analyses, I audited the flight activity data for data entry errors and missing data.

### **4.3. REVIEW OF THE VANTAGE POINT SURVEY COVERAGE AND RESULTS**

This collision risk model is based on the full GNM vantage point survey dataset, with the exception of data from VP8 and VP10. VP8 is not included, as there are no proposed turbine locations within the viewshed of that VP8, and the habitat covered by the viewshed is not representative of the wind farm site. VP10 is not included because it was only surveyed for two months. The vantage points included in the collision risk model are shown in Map 2.

Before beginning the development of the collision risk model, I carried out a review of the vantage point survey coverage and results. This helped to assess the degree of spatial and temporal variability in the recorded flight activity, which needed to be taken into account in the development of the collision risk model. This review is presented in the *Castlebanny Wind Farm, Co. Kilkenny: Ornithological Desk Review and Survey Report* (Gittings, 2020b). The requirements for adjustments to the Stage 1 model arising from the results of this review are discussed in Section 5.1. Note that, spatial and temporal variability can only be assessed for the regularly occurring species. With species that were only recorded occasionally, it is not possible to distinguish between sampling effects and true spatial and temporal variability.

### **4.4. COLLISION RISK MODELLING METHODOLOGY**

The collision risk modelling methodology is described in Sections 5-7 of this report as part of a step-by-step account of the development of the collision risk model.

## **5. COLLISION RISK MODEL STAGE 1: BIRD TRANSITS**

### **5.1. METHODOLOGY**

#### **5.1.1. General approach**

The stage 1 calculations use the vantage point survey data to calculate the predicted number of bird transits across the rotor swept volume. There are two methods described by SNH (2000) for carrying out stage 1 calculations: the “risk window” approach for when birds make regular flights through the flight risk area (e.g., geese commuting between roost sites and feeding areas); and the “bird occupancy” approach for when birds show variable patterns of flight activity within the flight risk area. I have used the “bird occupancy” approach, as this is generally the appropriate method for species that show variable patterns of flight activity, and the vantage point survey data and flightline mapping do not indicate regular flightlines through the wind farm site.

The sequential calculations that derive the predicted number of bird transits across the swept volume are shown in Table 5.1.

Table 5.1. Calculations of predicted number of bird transects across the rotor swept volume.

Step	Parameter	Calculation	Formula	Units	Details
1	t <sub>1</sub>	bird-secs observed at potential collision height / total duration of VP watches	$D_{bird}/VP_{eff}$	birds	Mean number of birds observed flying at rotor height during the vantage point watches
2	n	t <sub>1</sub> * total duration of season	$t_1 \times D_{season} \times 3600$	bird-secs	Predicted total number of birds observed flying at rotor height if the vantage point watches had covered the entire season
3	b	n × (volume swept by rotors / flight risk volume)	$n \times (A_{rotor} \times (L_{rotor} + L_{bird})) / (A_{vis} \times H_{rotor})$	bird-secs	Predicted bird occupancy of the swept volume across the entire season
4	N <sub>transits</sub>	b / time taken for a bird to fly through rotors of one turbine	$b / ((L_{rotor} + L_{bird}) / V_{bird})$	bird transits	Predicted number of transits across the swept volume across the entire season

Note: The SNH (2000) calculation procedure include additional steps, which calculate flight activity within the “risk area”, and then correct for the proportion of the risk area airspace occupied by the rotor swept volume of the turbines. However, these steps cancel out, so the calculation procedure shown in this table produces identical results.

The calculations in Table 5.1 simplify as Equation 1, as shown below.

$$\text{Equation 1: } (D_{bird} \times D_{season} \times N_{turb} \times A_{rotor} \times V_{bird}) / (H_{rotor} \times VP_{eff} \times A_{vis})$$

D<sub>bird</sub> = bird-secs observed at potential collision height, D<sub>season</sub> = total daylight hours across the season, N<sub>turb</sub> = number of turbines, A<sub>rotor</sub> = area of rotor discs, V<sub>bird</sub> = bird flight speed, H<sub>rotor</sub> = rotor diameter, VP<sub>eff</sub> = total duration of vantage point watches, and A<sub>vis</sub> = total area of viewshed.

Note that the rotor depth (L<sub>rotor</sub>) and bird length (L<sub>bird</sub>), which are included in the sequential calculations in Table 5.1, cancel out. While bird length is required for the collision probability calculations in stage 2, the rotor depth parameter (L<sub>rotor</sub>) is not usually required for collision risk modelling<sup>1</sup>.

### 5.1.2. Model types

In this assessment I have modelled the predicted transits for all species using three modelling approaches (the combined VP, VP averaging and turbine averaging methods). I also modelled the predicted transits for Lesser Black-backed Gull using a spatially structured version of the combined VP method. In addition, Kestrel flight activity during the vantage point survey was divided into direct flight and hovering components. I modelled the direct flight component using the above three modelling approaches, while I used a novel method to model the hovering component separately.

### 5.1.3. Viewshed analyses

#### ***Viewshed mapping***

I used contour data and measured, or estimated, heights of vegetation barriers, to draw viewshed maps for each VP, representing the area that was visible at 35 m above ground level (see Gittings, 2020b). However, analysis of the flightline mapping showed that were some sections of the mapped viewsheds in which no flight activity of any species was recorded. These were peripheral sections of the viewsheds, which the observers may not have focussed on in the surveys. Therefore, I clipped the mapped viewsheds to exclude these sections (Map 2).

There are three turbine locations which are outside any of the mapped viewsheds (Map 2). As these locations are only 55-70 m outside the nearest viewshed, the vantage point survey data from the nearest viewshed(s) can be considered to be representative of the likely flight activity at these locations. For the combined VPs and VP averaging models (see Section 5.2.1), the occurrence of turbine locations outside viewsheds does not affect the calculation procedure, as both models use the vantage point survey data to estimate the overall flight activity density across

<sup>1</sup> In this collision risk model, I have used rotor depth for the Hovering Kestrel Stage 1 model (see Section 5.2.3).

the wind farm site and then multiply by the total number of turbines. For the turbine averaging model (see Section 5.2.1) and the Lesser Black-backed Gull stage 1 model (see Section 5.2.2), these three turbines were allocated to the nearest viewshed.

### **Detection rates**

The analyses of the flightline mapping indicated that there was a decline in detection of flightlines with increasing distance from the vantage point location. I analysed this detection rate function, by dividing the viewsheds into 4 ha grid squares and counting the number of flightlines at potential collision height that intersected each grid square. I then calculated adjusted flightline densities for each grid square weighted by the overall number of flightlines recorded in the relevant viewshed:

$$\text{Equation 2: } FD_i^* = (FD_i / FD_{VP}) \times FD_{\text{mean}}$$

$FD_i^*$  = weighted flightline density in grid square  $i$ ;  $FD_i$  = raw flightline density in grid square  $i$ ;  $FD_{VP}$  = summed flightline densities across all grid squares in the viewshed containing grid square  $i$ ;  $FD_{\text{mean}}$  = mean of  $FD_{VP}$  = across all the vantage points included in the analysis.

I used the centroid of each grid square to calculate their distances from the vantage point location and calculated the weighted mean flightline density per grid square across all vantage points for 250 m distance bands from the vantage point location.

I carried out this analysis separately for both the GNM and MWP vantage point survey datasets, using flightlines for all species recorded in the datasets. I also carried out a separate analysis on Lesser Black-backed Gull flightlines in the GNM dataset, restricted to the high Lesser Black-backed Gull flight activity viewsheds (as defined in Section 5.2.2). For the analyses of the GNM dataset, I only included flightlines in the 35-135 m and > 135 m height bands. For the analysis of the MWP dataset, I only included flightlines in the 50-100 m, 100-200 m and > 200 m height bands.

Accurate viewshed mapping was not available for the MWP vantage points. Therefore, for the analysis of the MWP dataset, I included all flightlines within the viewshed arc of each vantage point, where the viewshed arc is defined as a 180° arc of radius 2 km. Then for the calculation of the weighted mean flightline density per grid square, I only used grid squares with a least one flightline intersection. This means that the analysis of the MWP dataset may overestimate the detection rates in the more distance bands due to the exclusion of grid squares with zero flightline intersections that were within the viewshed of the relevant vantage point.

The all species analyses of the GNM and MWP vantage point survey datasets showed very similar patterns of decline in detection rates with distance (Figure 5.1). The highest detection rate occurred in the 250-500 m distance band, with a steady decline in detection rate with increasing distance from the vantage point location. The slightly lower detection rate in the 0-250 m distance band could indicate some avoidance effect due to the presence of the surveyor at the vantage point location. However, the 0-250 m distance bands contained relatively small numbers of grid squares compared to the other distance bands, so there is a higher uncertainty about the estimates of the detection rate for this distance band (as indicated by the larger confidence intervals).

Compared to the all species analyses, the distance from the vantage point had a weaker effect on detection rates of Lesser Black-backed Gulls, with little decline in distance up to 1000 m, and a weaker decline beyond that distance. The detection rate of Lesser Black-backed Gulls in the 0-250 m distance band was relatively low, but there was a very wide confidence interval for this distance band. However, the apparent decline in detectability for Lesser Black-backed Gull may be partly due to real differences in Lesser Black-backed Gull flight activity: considering the overall pattern of flightlines across the GNM and MWP datasets, it seems likely that higher concentrations of flight activity would be expected close to several of the GNM vantage points, even allowing for the exclusion of the low flight activity viewsheds.

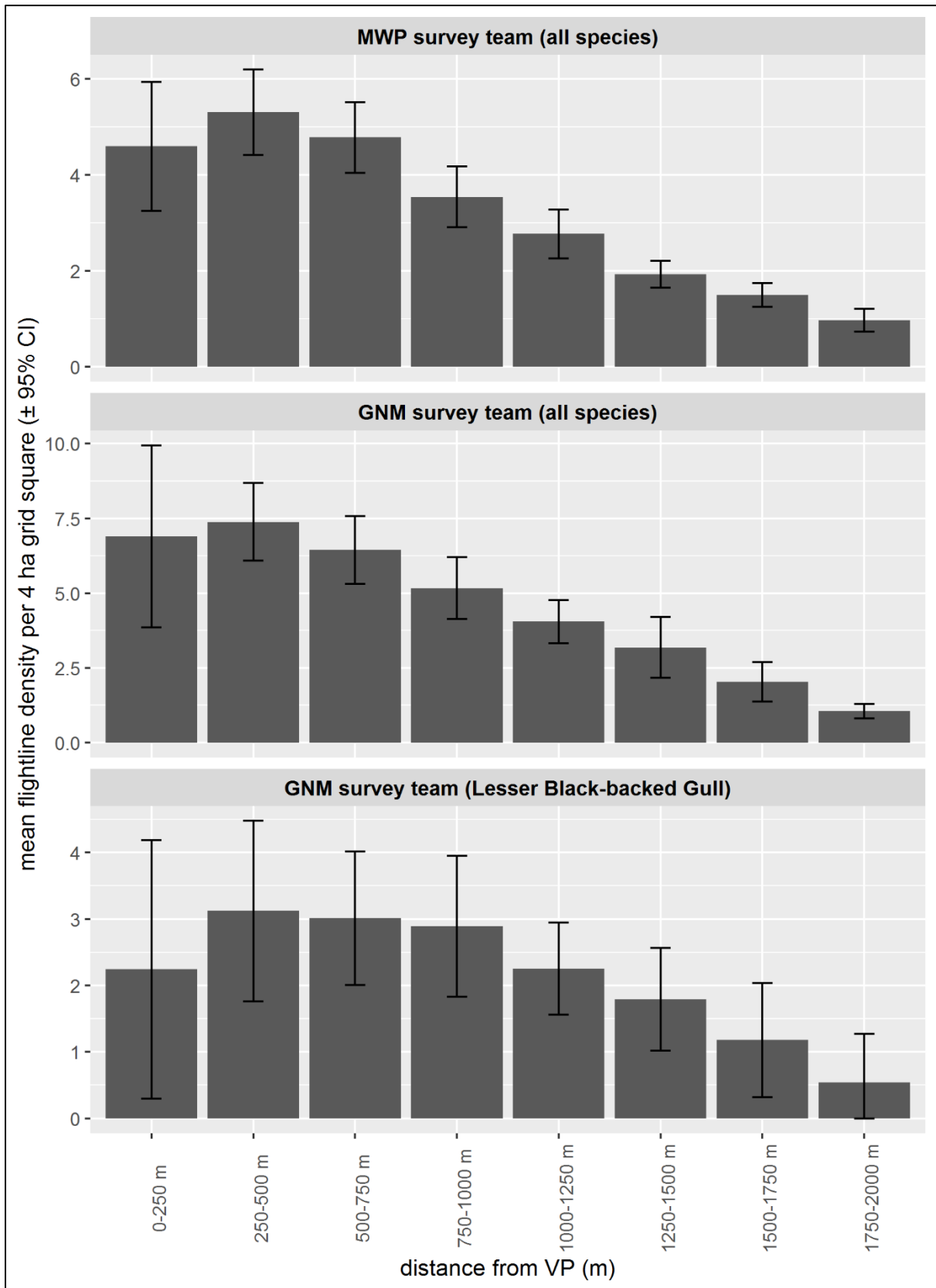


Figure 5.1. Relationship between density of flightlines at potential collision height and distance from vantage point location, using data from all species across all vantage points, weighted by total number of flightlines at potential collision height recorded at each vantage point.

As the GNM and MWP surveys were carried out by independent teams of observers, using different vantage point locations, this decline in detection rate is unlikely to be an artefact of the habitats within the particular viewsheds. Therefore, I used the detection rate / distance relationships in the analyses of the GNM dataset to calculate adjusted viewshed areas using the formula shown in Equation 3.

Equation 3:  $A_{vis}^* = \sum_{i=1-8} (A_{vis(i)} \times \text{weight}_i)$

$A_{vis}^*$  = adjusted viewshed area;  $i$  = distance band number from 0-250 m (distance band 1) to 1750-2000 m (distance band 8);  $\text{weight}_i$  = mean detection rate in distance band  $i$  relative to the 250-500 m distance band.

### **Re-calculation of flight durations**

As some mapped flightlines extended outside the viewshed boundaries, I clipped the mapped flightlines by the viewsheds, and recalculated the flight durations and bird-secs by multiplying their original values by (clipped flightline length)/(original flightline length).

#### **5.1.4. Height bands**

##### **Adjustment of flight activity data**

The vantage point survey used a height band of 35-135 m to represent the potential collision height band. However, the potential collision height band for the turbine model used for this collision risk model is 30-185 m. Therefore, I needed to estimate the additional flight activity that occurred in the 30-35 m and 135-185 m height bands.

For the 135-185 height band, I simply made the precautionary assumption that all flight activity recorded above 135 m was within this height band. The total amount of flight activity recorded above 135 m was low (less than 3% of the bird-secs recorded within the 35-135 m height band), so any inclusion of flight activity above 185 m by this procedure will not have significantly affected the calculated collision risks.

For the 30-35 m height band, I used separate calculation procedures to estimate the additional flight activity depending on the nature of the vantage point survey data that was available for the 0-35 m height band for each species.

For species for which flight durations were recorded for all flights in the 0-35 m height band, I multiplied the recorded bird-secs by 2/7 to estimate the proportion in the 30-35 m height band. This factor represents the proportion of the 0-35 m height band occupied by the 30-35 m height band, multiplied by 2 in case there is uneven distribution of flight activity within the 0-35 m height band.

For Lesser Black-backed Gull, I calculated the mean seconds per metre for all mapped flightlines where the total flight duration was recorded and then used this parameter to estimate durations from the flightline lengths for records where duration was not recorded for the 0-35 m height band. If the record included flight activity at higher height bands, I subtracted the recorded durations from these height bands to obtain the estimated duration at the 0-35 m height band.

For Sparrowhawk, Buzzard, and Kestrel, I did not consider that estimation of duration from flightline lengths would be reliable, as their flight activity involved a lot of repeated circling and (for Kestrel) hovering. For these species, I first used data from records where all flight durations were recorded to calculate the proportion of bird-secs that occurred in the 0-35 m height band ( $p_{0-35}$ ). I then estimated the flight activity in the 30-35 m height band ( $D_{\text{bird}(30-35)}$ ), using the recorded flight activity in the 35-135 m height band ( $D_{\text{bird}(35-135)}$ ) using the following equation:

Equation 4:  $D_{\text{bird}(30-35)} = D_{\text{bird}(35-135)} \times p_{0-35} \times 2/7$

##### **Calculation of rotor area**

I carried out separate calculations of bird transits for each height band (30-35 m, 35-135 m, and 135-185 m). This allowed the differences in the rotor area as a proportion of the airspace to be factored into the calculations and reduced any effect of errors in the estimation of the flight activity

within the 30-35 m height band<sup>2</sup>. To carry out these separate calculations, it was necessary to subdivide the overall rotor area ( $A_{rotor}$ ) into the portions that occurred in each height band. To calculate the rotor area in each height band, I first calculated the angles subtended by segments representing the 25-35 m and 35-50 m height bands using the following equations:

$$\text{Equation 5: } \theta_{35} = \cos^{-1} ((H_{hub} - 35) / R_{rotor})$$

$$\text{Equation 6: } \theta_{50} = \cos^{-1} ((H_{hub} - 50) / R_{rotor})$$

$H_{hub}$  = hub height;  $R_{rotor}$  is the rotor radius.

I then calculated the rotor areas using the following equations:

$$\text{Equation 7: } A_{rotor(25-35)} = 0.5 \times (\theta_{35} - \sin(\theta_{35})) \times R_{rotor}^2$$

$$\text{Equation 8: } A_{rotor(35-50)} = A_{rotor(25-35)} - (0.5 \times (\theta_{50} - \sin(\theta_{50})) \times R_{rotor}^2)$$

$$\text{Equation 9: } A_{rotor(50-170)} = A_{rotor} - (A_{rotor(25-35)} + A_{rotor(35-50)})$$

Similarly, I adjusted the rotor height ( $H_{rotor}$ ) value for each height band to equal the height of the height band.

### 5.1.5. Vantage point survey effort

The overall survey effort varied between vantage points. Therefore, for models that combined data from more than one vantage point, I used the following equation to standardise the vantage point survey effort:

$$\text{Equation 10: } VP_{eff}^* = \sum_{(i=1 \text{ to } n)} (VP_{eff(i)} \times A_{vis}^*(i)) / \sum_{(i=1 \text{ to } n)} (A_{vis}^*(i))$$

$VP_{eff}^*$  = the standardised vantage point survey effort;  $n$  = the number of vantage points grouped together for the analysis;  $VP_{eff(i)}$  = the vantage point survey effort at  $VP_i$ ;  $A_{vis(i)}$  = the adjusted viewshed area at  $VP_i$  (see Equation 3).

### 5.1.6. Parameter values

The parameter values used in the calculations of predicted transits are shown in Appendix 1.

### 5.1.7. Definition of seasonal periods of occurrence

In developing a collision risk model it is important to consider seasonal patterns of occurrence for two reasons. Firstly, if a species has more than one population using the wind farm site (e.g., a wintering population that is distinct from the breeding population), separate collision risks need to be calculated so that the impact on each population can be assessed. Secondly, the  $D_{season}/VP_{eff}$  ratio in Equation 1 (Section 5.1.1) means that if a species has uneven patterns of seasonal occurrence, the calculation of predicted transits may be biased, assuming that the monthly survey effort was not proportional to daylength (which will usually be the case).

I used the results of the analysis of the vantage point survey data (Gittings, 2020b) for the regularly occurring species, and knowledge of the general occurrence patterns of the species in Ireland, for all the species, to define seasonal periods of occurrence for all the species included in the collision risk model. These seasonal periods of occurrence are shown in Table A1.6 in Appendix 1.

For Lesser Black-backed Gull, the division into four seasonal periods helps to distinguish between the collision risk in the main breeding season period when visiting birds from the Saltee Islands colony may form a high proportion of the adult Lesser Black-backed Gull flight activity, and the autumn migration period when these birds will be swamped by the much larger numbers of birds in the populations that migrate through Ireland. The rationale for the definition of the Lesser Black-backed Gull seasonal occurrence periods is discussed in more detail in Gittings (2020a).

The other three species that regularly occurred during the vantage point surveys (Sparrowhawk, Buzzard and Kestrel) are resident at the wind farm site. The analysis of the vantage point survey data (Gittings, 2020b), showed seasonal differences in Sparrowhawk and Buzzard occurrence patterns, but no consistent seasonal differences in Kestrel occurrence patterns. However, the

<sup>2</sup> The use of separate rotor areas for each height band causes a more than three-fold reduction in the influence of the flight activity data from the 30-35 m height band.

seasonal differences in Sparrowhawk overall occurrence patterns was not reflected in the level of flight activity at potential collision height. With Buzzard, the peak seasonal occurrence period was in February-May was centred around the spring equinox, with more or less uniform seasonal occurrence patterns outside this period. Hence, there was no need to correct for seasonal variation in occurrence patterns to prevent bias in calculation of predicted transits as, during the peak occurrence period, the reduction in the  $D_{\text{season}}/VP_{\text{eff}}$  ratio before the spring equinox was compensated by the increase in this ratio after the spring equinox. Therefore, as Sparrowhawk, Buzzard and Kestrel have resident populations at the wind farm site, and as there was no need for seasonal subdivision to prevent bias in the model, the collision risk models for these species were not divided into separate seasonal periods.

#### **5.1.8. Diel variation in flight activity**

If species show diel variation in flight activity, the calculation of predicted transits will be biased if the vantage point survey effort is not evenly spread throughout the day. The latter is difficult to achieve, due to overlap effects (survey periods can overlap in the middle of the day, but cannot overlap in the early morning and evening, due to the constraints of starting at sunrise and finishing at sunset).

The vantage point surveys that provided the data for this collision risk model covered the full sunrise to sunset period, but there was a higher survey intensity during the middle of the day compared to the early morning and late evening (Gittings, 2020b). Of the four regularly occurring species, Sparrowhawk and Lesser Black-backed Gull did not show any consistent patterns of diel variation in flight activity, while Buzzard showed higher levels of activity during the morning, compared to the afternoon and evening, and Kestrel showed higher levels of activity during the morning and afternoon, compared to the evening (Gittings, 2020b). Therefore, as the highest levels of Buzzard and Kestrel flight activity occurred during diel periods with high intensities of survey effort, the diel variation in their flight activity will not cause underestimation of the collision risk, but might cause overestimation. However, as any overestimation will be slight due to the pattern of the diel variation in flight activity compared to the diel variation in vantage point survey effort, I did not consider that any adjustment to the collision risk model was required.

### **5.2. MODELLING METHODOLOGY AND RESULTS**

#### **5.2.1. General models**

The basic mathematical method for calculating predicted transits using the occupancy method (as described in Section 5.1.1) is explained by SNH (2000), and, in any case, can be easily derived from first principles. However, SNH (2000) does not provide guidance on how to incorporate data from multiple vantage points in calculations of predicted transits. The simplest method (the combined VPs method) combines the data from all the vantage points, using the sum of the flight activity across all the vantage points for the  $D_{\text{bird}}$  value, and the sum of the viewshed areas for the  $A_{\text{vis}}$  value. This method assumes that flight activity is randomly distributed throughout the combined viewsheds.

The predicted transits calculated using this method are shown in Table 5.2.

Table 5.2. Predicted transits per year using the combined VPs method.

Species	Transits per height band			Total predicted transits / year
	30-35 m	35-135 m	135-185 m	
Mallard	2	89	0	91
Cormorant	0	12	0	12
Grey Heron	6	29	0	36
Hen Harrier	1	5	0	6
Sparrowhawk	9	146	12	167
Buzzard	75	1,402	177	1,654
Golden Plover	4	77	0	81
Lapwing	0	56	0	56
Whimbrel	10	12	0	23
Curlew	104	36	0	139
Black-headed Gull	<1	13	9	23
Lesser Black-backed Gull (spring)	76	76	0	152
Lesser Black-backed Gull (breeding)	108	3,021	238	3,367
Lesser Black-backed Gull (autumn)	168	5,441	63	5,672
Lesser Black-backed Gull (winter)	1	6	0	7
Herring Gull	0	9	0	9
Kestrel	210	892	28	1,131
Peregrine	3	74	0	77

Predicted transits for Kestrel are for birds in direct flight only; see Section 5.2.3 for predicted transits of hovering Kestrel.

A slightly more sophisticated method is the VP averaging method. This involves calculating predicted transits per turbine separately for each vantage point and then using the mean predicted transits/turbine across all vantage points to calculate the overall number of transits predicted across the entire wind farm site. This method is widely used (in Ireland) and has also been taught at courses on collision risk modelling run by the Chartered Institute of Ecology and Environmental Management. This method also assumes that there is random distribution of flight activity across the wind farm site, but treats each vantage point as a separate sample. The predicted transits calculated using this method are shown in Table 5.3. Note that the calculations of the overall mean transits per turbine for Hen Harrier, Golden Plover and Lesser Black-backed Gull (winter) excluded VP7 as that vantage point was only surveyed for two winter months.

If there is significant spatial structure in the flight activity patterns, then both the above methods will produce biased estimates of predicted transits. A simple way to incorporate spatial structure is to use the predicted transits per turbine calculated for each vantage point to allocate predicted transits for each individual turbine, and then sum the predicted transits across all the turbines (the turbine averaging method). Where a turbine occurs in the viewshed of more than one vantage point, the predicted transits for that turbine is the mean of the predicted transits per turbine for the relevant vantage points. This method still assumes that there is random distribution of flight activity within each viewshed, and also assumes that variation in recorded flight activity between the vantage points reflects real spatial variation in flight activity across the site, not sampling error. Therefore, this method is more appropriate for species with relatively high levels of recorded flight activity. The predicted transits calculated using this method are shown in Table 5.4.

Table 5.3. Predicted transits using the VP averaging method.

Species	Transits/turbine								Total predicted transits/year
	VP1	VP2	VP3	VP4	VP5	VP6	VP7	VP9	
Mallard	0	0	0	0	17	0	0	0	43
Cormorant	0	0	0	0	0	7	0	0	19
Grey Heron	0	0	0	0	6	0	0	0	17
Hen Harrier	<1	0	0	0	1	0	0	0	4
Sparrowhawk	7	6	1	16	4	30	0	2	172
Buzzard	40	4	137	215	40	36	89	0	1,478
Golden Plover	0	0	0	2	15	0	0	0	44
Lapwing	0	0	22	0	0	0	0	0	57
Whimbrel	3	20	0	0	0	0	0	1	65
Curlew	0	0	142	0	0	0	0	30	450
Black-headed Gull	0	0	4	4	0	0	0	0	19
Lesser Black-backed Gull (spring)	0	0	0	0	9	0	117	0	331
Lesser Black-backed Gull (breeding)	1	0	200	255	9	33	20	1,740	5,930
Lesser Black-backed Gull (autumn)	0	0	78	574	343	0	18	1,332	6,158
Lesser Black-backed Gull (winter)	0	0	1	1	0	0	0	0	6
Herring Gull	0	0	3	0	0	0	0	0	9
Kestrel	20	38	119	89	45	4	71	29	1,090
Peregrine	0	0	3	12	6	0	0	0	56

Predicted transits for Kestrel are for birds in direct flight only; see Section 5.2.3 for predicted transits of hovering Kestrel. The calculations of the overall mean transits per turbine, which were then used to calculate the total predicted transits/year for Hen Harrier, Golden Plover and Lesser Black-backed Gull (winter) excluded VP7 (see text).

Table 5.4. Comparison of predicted transits between the combined VPs, VP averaging, and turbine averaging methods.

Species	Total predicted transits/year		
	combined VPs method	VP averaging method	turbine averaging method
Mallard	91	43	58
Cormorant	12	19	18
Grey Heron	36	17	23
Hen Harrier	6	4	6
Sparrowhawk	167	172	177
Buzzard	1,654	1,478	1,812
Golden Plover	81	44	57
Lapwing	56	57	98
Whimbrel	23	65	26
Curlew	139	450	668
Black-headed Gull	23	19	28
Lesser Black-backed Gull (spring)	152	331	208
Lesser Black-backed Gull (breeding)	3,367	5,930	3,557
Lesser Black-backed Gull (autumn)	5,672	6,158	4,635
Lesser Black-backed Gull (winter)	7	6	0
Herring Gull	9	9	15
Kestrel	1,131	1,090	1,214
Peregrine	77	56	71

Predicted transits for Kestrel are for birds in direct flight only; see Section 5.2.3 for predicted transits of hovering Kestrel.

### 5.2.2. Lesser Black-backed Gull stage 1 model

In the comparison in Table 5.4 the VP averaging method produces much larger estimates of predicted transits for Lesser Black-backed Gull in the breeding season and the autumn than either the combined VPs or turbine averaging methods. This is due to the large amount of flight activity in VP9, which was mainly due to single records involving large flocks of Lesser Black-backed Gulls in each season. This produced a high estimate of flight activity density, which increased the overall mean transits/turbine across the site. The spatial structure incorporated in the turbine averaging method, downweights the influence of VP9 as its viewshed only contains a single turbine. However, due to the rarity of their occurrence, there was likely to be a high degree of sampling error in the recording of the distribution of large flocks of Lesser Black-backed Gulls between vantage points. Therefore, for Lesser Black-backed Gull, there may have been a significant violation of the assumption in the turbine averaging method that the variation between vantage points in recorded flight activity patterns represents real variation between vantage points. Instead, for more realistic modelling of spatial structure in Lesser Black-backed Gull flight activity patterns, I used an adaptation of the combined VPs method. This involved dividing the wind farm site into areas of high and low Lesser Black-backed Gull flight activity and using the combined VPs method to calculate predicted transits separately in each area. The division between the high and low Lesser Black-backed Gull flight activity was largely based on vantage point viewsheds, but the viewsheds of vantage points 4, 5 and 7 were subdivided to reflect the concentration of Lesser Black-backed Gull flight activity along the lower ground in these viewsheds (Map 3). This model produced estimates of 122 transits/year in spring, 2,689 transits per year in the breeding season, 4,966 transits per year in autumn, and 6 transits per year in winter.

### 5.2.3. Hovering Kestrel stage 1 model

The equation for calculating predicted transits using the models described above (Equation 1) includes the mean bird flight speed as part of the numerator. However, for Kestrel, a significant proportion of their flight activity will typically involve hovering birds. The flight speed of a hovering Kestrel is close to zero (a small amount of drift in position will often occur during long bouts of hovering). Therefore, using the mean flight speed for Kestrel (10.1 m/sec; Alerstam et al., 2007) in Equation 1 to predict transits of hovering Kestrel is clearly inappropriate and will result in highly inflated estimates.

In the vantage point survey for this assessment, all Kestrel flight records were categorised as predominantly direct flight, or predominantly hovering. In addition, in a sample of 13 hovering flights, the number of hovering bouts, and the duration of each hovering bout, was timed. This allowed estimation of the mean proportion of hovering flight ( $p_h$ ), and the mean number of hovering positions per second ( $P_{hov}$ ), in the flight records categorised as involving predominantly hovering. The estimated direct flight component of the hovering flight records ( $1 - p_h$ ) was added to the flight activity from the direct flight records to give the bird-mins ( $D_{bird}$ ) included in the basic models. The estimated hovering component of the hovering flight records was used in a separate model, described below, to calculate predicted transits for hovering Kestrel.

As hovering Kestrel are essentially stationary, the number of transits are simply a function of the number of separate positions hovering Kestrel occupy over the season. This can be calculated using Equation 11, as shown below.

Equation 11:  $(D_{bird(hov)} \times p_h \times P_{hov} \times D_{season} \times N_{turb} \times H_{rotor} \times W_{rotor}) / (VP_{eff} \times A_{vis})$

$D_{bird(hov)}$  = bird-secs observed at potential collision height (records classified as predominantly hovering flight);  $p_h$  = mean proportion of hovering in records classified as predominantly hovering flight;  $P_{hov}$  = hovering positions per second;  $D_{season}$  = total daylight hours across the season;  $N_{turb}$  = number of turbines;  $H_{rotor}$  = rotor diameter;  $W_{rotor}$  = rotor depth;  $VP_{eff}$  = total duration of vantage point watches; and  $A_{vis}$  = total area of viewshed.

Using this Equation 11, the total predicted transits of hovering Kestrels was 36 transits/year.

## 6. COLLISION RISK MODEL STAGE 2: COLLISION PROBABILITY

### 6.1. METHODOLOGY

Stage 2 of the collision risk model involves calculating the probability of a collision when a bird makes a transit of the rotor swept volume.

The Scottish Natural Heritage collision risk model (SNH, 2000; Band *et al.*, 2007; Band, 2012) calculates the probability,  $p(r, \varphi)$ , of collision for a bird at radius  $r$  from the hub and at a position along the radius that is at angle  $\varphi$  from the vertical. This probability is then integrated over the entire rotor disc, assuming that the bird transit may be anywhere at random within the area of the disc. Separate calculations are made for flapping and gliding birds and for upwind and downwind transits. This method assumes that: birds are of a simple cruciform shape, fly through turbines in straight lines with a perpendicular approach to the plane of the rotor, and their flight is not affected by the slipstream of the turbine blade; and that turbine blades have width and pitch angle, but no thickness.

The collision probability calculations for the original Scottish Natural Heritage collision risk model can be carried out using an Excel spreadsheet which is provided as an accompaniment to the SNH (2000) guidance. This spreadsheet was updated by Band (2012) by changing the details of the blade profile used in the model<sup>3</sup>. The updated model is included in R code provided by Masden (2015). For the present assessment, I adapted R code from that provided by Masden (2015) to

<sup>3</sup> Note that, strictly speaking, the model should be adapted for each turbine specification by changing the details of the blade profile in the model to match the blade profile of the turbine. However, in practice, this would make very little difference to the predicted collision risk, and the details of the blade profile are usually not available.

carry out the collision probability calculations. I audited this R code audited against the Band (2012) spreadsheet to confirm that it produced matching collision probability calculations.

One of the turbine parameters used to calculate collision probability is the mean pitch angle of the turbine blade. This parameter specifies the angle of the blade from the horizontal, so the collision probability will increase as the mean pitch angle increases. Data on mean pitch angle can be difficult to obtain so generic values are often used in collision risk models. These are often based on the statement by Band (2012) that a mean pitch angle of “25-30 degrees is reasonable for a typical large turbine”. However, Band was referring to offshore wind farms where wind speeds are higher than at onshore wind farms, resulting in higher mean pitch angles. For this assessment, I applied a more realistic scenario from an onshore wind farm (Meenwaun, Co. Offaly). The pitch angle over a continuous 12 month period at this site was for approximately 90% of the time between -3° and 9° (MKOS, 2019). I used the maximum value from this range (9°) for the collision probability calculations. For comparison, I also calculated collision probabilities using a mean pitch angle of 27.5°.

Another turbine parameter used to calculate collision probability is the rotation speed of the turbine blades. I used data on the relationship between wind speed and the turbine rotation speed from the turbine specifications, and wind speed data from Kilkenny weather station, to calculate mean rotation speed values to use for each species/population, based on their seasonal periods of occurrence, as shown in Table A1.6.

The parameter values used in the calculations of collision probability are shown in Appendix 1.

## **6.2. RESULTS**

The results of the collision probability calculations are shown in Table 6.1. Using a 9° mean pitch value, the probabilities range from 4.6% for Whimbrel to 8.6% for Hen Harrier but the differences between the probabilities for flapping and gliding flight are negligible. The 27.5° mean pitch value increases the collision probabilities, with the increases ranging from 1.0% (Mallard) to 3.2% (Hen Harrier). Across all the species, the magnitudes of the increases are a logarithmic function of the species flight speeds:  $\text{increase} = -0.03 \times \ln(\text{flight speed}) + 0.0957$ ;  $r^2 = 0.96$ .

Table 6.1. Collision probabilities calculated using mean pitch values of 9° (from a comparable onshore wind farm) and 27.5° (representative of a typical large turbine in an offshore wind farm).

Species	9° mean pitch			27.5° mean pitch
	flapping	gliding	mean	mean
Mallard	4.9%	4.8%	4.8%	5.9%
Cormorant	6.5%	6.3%	6.4%	8.0%
Grey Heron	7.8%	7.5%	7.7%	9.8%
Hen Harrier	8.7%	8.5%	8.6%	11.9%
Sparrowhawk	5.8%	5.7%	5.7%	8.1%
Buzzard	6.6%	6.4%	6.5%	8.8%
Golden Plover	5.7%	5.4%	5.6%	6.9%
Lapwing	5.3%	5.1%	5.2%	7.2%
Whimbrel	4.7%	4.5%	4.6%	5.9%
Curlew	5.2%	5.1%	5.1%	6.5%
Black-headed Gull	5.9%	5.7%	5.8%	8.0%
Lesser Black-backed Gull (spring)	6.3%	6.0%	6.2%	8.2%
Lesser Black-backed Gull (breeding)	5.9%	5.6%	5.7%	7.4%
Lesser Black-backed Gull (autumn)	6.0%	5.7%	5.9%	7.7%
Lesser Black-backed Gull (winter)	6.4%	6.1%	6.2%	8.3%
Herring Gull	5.9%	5.8%	5.8%	7.9%
Kestrel	6.4%	6.3%	6.3%	9.1%
Peregrine	6.0%	5.8%	5.9%	8.1%

## 7. COLLISION RISK MODEL STAGE 3: COLLISION PREDICTION

Stage 3 of the collision risk model uses the predicted transits from stage 1 and the collision probabilities from stage 2 to calculate the predicted collisions. However, three further factors need to be considered: the proportion of time the wind farm is operational; the avoidance rate; and the degree of any nocturnal flight activity.

Wind turbines in operational wind farms will have periods when they are not turning due to maintenance or wind speeds. Therefore, the predicted collisions need to be corrected by the percentage of time the wind turbines will be operational.

The avoidance rate reflects the fact that most potential collisions are avoided due to birds taking evasive action (SNH, 2010). This avoidance rate includes both behavioural avoidance (micro-avoidance) and behavioural displacement (macro-avoidance). Behavioural avoidance is “action taken by a bird, when close to an operational wind farm, which prevents a collision”. Behavioural displacement refers to the process by which a “bird may (possibly over time) change its home range, territory, or flight routes between roosting areas and feeding areas, so that its range use (or flight paths) no longer bring the bird into the vicinity of an operational wind farm”. Scottish Natural Heritage provides guidance on avoidance rates to use in collision risk assessments (SNH, 2010, 2018). For some species, including Hen Harrier and Kestrel, there is some evidence available that has been used to specify species-specific avoidance rates (SNH, 2018). In addition, a recent review for Scottish Natural Heritage has recommended the use of an avoidance rate of 0.995 for large gulls (including Lesser Black-backed Gull) at onshore wind farms (Furness, 2019). For the other species included in this collision risk model, the SNH guidance specifies a default avoidance rate of 98%.

Another factor that needs to be considered is the degree of nocturnal flight activity that is likely to occur. The calculations of predicted transits are based on flight activity during daylight hours only. Therefore, if a species is likely to have a significant amount of nocturnal flight activity, a correction should be made to account for this nocturnal flight activity. Of the species, included in this assessment, only Grey Heron, Golden Plover and Lapwing are likely to have significant levels of nocturnal flight activity. For Golden Plover, a figure of 25% of the day-time activity levels across the night-time hours is often used in collision risk modelling (e.g., MKOS, 2019). Lapwing show similar patterns of flight activity, while flight activity patterns for Grey Heron from Vessem and Draulans (1987) indicate low levels of nocturnal flight activity. Therefore, I have used this figure in this assessment for all three of the above species, in the absence of any other data. I calculated the correction factor using the following equation:

Equation 12:  $NCF = 1 + 0.25 \times h_{\text{night}} / h_{\text{day}}$

NCF = correction factor for nocturnal flight activity;  $h_{\text{night}}$  = mean night-time hours across seasonal period of occurrence;  $h_{\text{day}}$  = mean day-time hours across seasonal period of occurrence.

This formula gave correction factors of 1.24 for Grey Heron, 1.34 for Golden Plover and 1.24 for Lapwing.

The predicted transits for Kestrel used for the collision predictions included two components: the predicted transits from the turbine averaging model for the direct flight component; and the predicted transits from the Hovering Kestrel Stage 1 model for the hovering flight component. However, the calculated collision probability only applies to the direct flight component, as it uses a mean flight speed representative of direct flight activity. Transits of hovering Kestrel can be assumed to have a collision probability of 100%, as the duration of a single hovering bout will be much longer than the interval between successive sweeps of turbine blades.

The calculation procedure to obtain the predicted collisions is summarised in the following equation:

Equation 13: predicted collisions =  $(\text{transits}_{\text{df}} \times p_{\text{coll}} + \text{transit}_{\text{hov}}) \times AR \times OP \times NCF$

$\text{transits}_{\text{df}}$  = predicted transits (direct flight activity);  $\text{transit}_{\text{hov}}$  = predicted transits (hovering flight activity);  $p_{\text{coll}}$  = collision probability; AR = avoidance rate; OP = Percentage of time the turbines will be operational; NCF = correction factor for nocturnal flight activity

The results of the stage 3 calculations are shown in Table 7.1 as the predicted number of collisions per year, and the total number of collisions predicted over the nominal 35 year lifespan of the wind farm. The species with the highest predicted collisions were Sparrowhawk, Buzzard, Curlew, Lesser Black-backed Gull (summer) and Kestrel. For Sparrowhawk, Buzzard, and Kestrel, this reflects the presence of sizeable resident populations within the wind farm site, while for Lesser Black-backed Gull, this reflects the occurrence of a regular commuting route across the site and exploitation of fields around the edge of the site. The Curlew collision risk is mainly due to records of two flocks during one vantage point watch in August 2017. These flocks were flying below the potential collision height band (35-135 m) that was used for the vantage point survey, but a proportion of their flight activity was allocated to the 30-35 m height band for the collision risk modelling. The predicted collision risk is negligible for all the other species included in the model. The separate modelling of the direct flight and hovering components of K flight activity caused a significant reduction in the predicted collision risk: if the hovering component had been included in the turbine averaging model, the predicted collision risk would have been around three times higher.

Table 7.1. Predicted number of collisions/year and predicted number of collisions over the 35 year lifespan of the wind farm.

Species	Predicted transits	Avoidance rate	Collision probability	Collisions/year	Collisions/ 35 years
Mallard	67	98.0%	4.8%	0.06	1.9
Cormorant	16	98.0%	6.4%	0.02	0.6
Grey Heron	26	98.0%	7.7%	0.04	1.5
Hen Harrier	5	99.0%	8.6%	0.004	0.1
Sparrowhawk	177	98.0%	5.7%	0.17	6.1
Buzzard	1,812	98.0%	6.5%	2.0	70
Golden Plover	62	98.0%	5.6%	0.08	2.8
Lapwing	56	98.0%	5.2%	0.06	2.2
Whimbrel	44	98.0%	4.6%	0.03	1.2
Curlew	295	98.0%	5.1%	0.26	9.0
Black-headed Gull	21	99.2%	5.8%	0.01	0.3
Lesser Black-backed Gull (spring)	122	99.5%	6.2%	0.03	1.1
Lesser Black-backed Gull (breeding)	2,689	99.5%	5.7%	0.7	23
Lesser Black-backed Gull (autumn)	4,966	99.5%	5.7%	1.2	43
Lesser Black-backed Gull (winter)	6	99.5%	5.9%	0.002	0.1
Herring Gull	9	98.0%	6.2%	0.01	0.3
Kestrel	1,250	95.0%	5.8%	4.8	169
Peregrine	67	98.0%	6.3%	0.07	2.3

Avoidance rates from SNH (2018) and Furness (2019). Collision probability estimates are from the calculations that used mean pitch values of 9°. Predicted transits are from the turbine averaging model for Sparrowhawk, Buzzard and Kestrel, with additional transits added from the Hovering Kestrel stage 1 model, and from the Lesser Black-backed Gull stage 1 model for Lesser Black-backed Gull (summer). For all the other species, the predicted transits are the mean of the values from the combined VPs and VP averaging models. The predicted collisions include a correction for the percentage of operational time (85%). The predicted collisions for Grey Heron, Golden Plover and Lapwing include a correction for nocturnal flight activity (see text). The calculation of the predicted collisions for Kestrel assumed a collision probability of 100% for hovering Kestrel (see text).

## 8. CONCLUSIONS

In this collision risk model, I have used three methods to predict the collision risk for all the species included in the modelling. The combined VPs and VP averaging methods assume random distribution of flight activity across the site. These methods are appropriate for species with low levels of recorded flight activity, where it is not possible to detect spatial structure from the vantage point survey data, and where spatially structured models might be strongly biased by sampling effects. The turbine averaging method incorporates spatial structure at the scale of the vantage point viewshed. I consider this to be the most appropriate method for Buzzard, Sparrowhawk and Kestrel, as this scale is likely to reflect the spatial structure of their populations within the wind farm site, and the model is unlikely to be strongly biased by sampling effects. I used a separate model to accommodate the spatial structure in the Lesser Black-backed Gull flight activity, while I also carried out a separate modelling exercise for the hovering component of Kestrel flight activity. Comparison of the results of the different models shows that decisions made during the modelling process can have significant effects on the predicted collision risk, and indicate that basic models, which do not incorporate spatial structure, may produce biased estimates for species with high levels of flight activity.

The only species with non-negligible collision risks were Sparrowhawk, Buzzard, Curlew, Lesser Black-backed Gull and Sparrowhawk. For Curlew, this may have been an artefact of the procedure used to estimate flight activity in the 30-35 m height band. For the other species, this reflects the occurrence of resident populations, or regular commuting routes, within, or across, the wind farm

site. The significance of the predicted collision risks are assessed in the Ornithology chapter of the *Castlebanny Wind Farm Environmental Assessment Report*. As part of that assessment, the level of uncertainty in the collision risk prediction is discussed: i.e., what is the likely upper bound of the confidence interval around the predicted collision risk.

## REFERENCES

- Alerstam, T., Rosén, M., Bäckman, J., Ericson, P.G.P. & Hellgren, O. (2007). Flight speeds among bird species: allometric and phylogenetic effects. *PLoS Biol*, 5, e197.
- Band, B. (2012) *Using a Collision Risk Model to Assess Bird Collision Risks for Offshore Windfarms. Guidance document*. SOSS Crown Estate.
- Band, W., Madders, M., & Whitfield, D.P. (2007). Developing field and analytical methods to assess avian collision risk at wind farms. In: de Lucas, M., Janss, G.F.E. & Ferrer, M. (eds.) *Birds and Wind farms: Risk Assessment and Mitigation*, pp. 259-275. Quercus, Madrid.
- Furness, R.W. (2019). Avoidance Rates of Herring Gull, Great Black-Backed Gull and Common Gull for Use in the Assessment of Terrestrial Wind Farms in Scotland. *Scottish Natural Heritage Research Report No. 1019*. Scottish Natural Heritage.
- Gittings, T. (2020a). *Castlebanny Wind Farm, Co. Kilkenny: Literature review, analyses of GPS tracking data, and analyses of vantage point survey data from the Castlebanny Wind Farm project, to inform the assessment of collision risk to the Saltee Islands Lesser Black-backed Gull population*. Included as Appendix 8 of the Ornithology chapter in the Castlebanny Wind Farm Environmental Impact Assessment Report.
- Gittings, T. (2020b). *Castlebanny Wind Farm, Co. Kilkenny: Ornithological Desk Review and Survey Report*. Included as Appendix 1 of the Ornithology chapter in the Castlebanny Wind Farm Environmental Impact Assessment Report.
- Masden, E. (2015). *Developing an Avian Collision Risk Model to Incorporate Variability and Uncertainty. Scottish Marine and Freshwater Science Vol 6 No 14*. Scottish Government, Edinburgh.
- MKOS (2019). *Cushaling Windfarm Site, Co. Offaly/Kildare: Collision Risk Assessment*. Unpublished report included as an appendix to the Cushaling Windfarm Environmental Impact Assessment Report. McCarthy Keville O'Sullivan Ltd., Galway.
- MWP (2019a). *Ornithology Report, Castlebanny, Mullinavat, Co. Kilkenny, Winter 2017/18*. Included in Appendix 2 of the Ornithology chapter in the Castlebanny Wind Farm Environmental Impact Assessment Report.
- MWP (2019b). *Ornithology Report, Castlebanny, Mullinavat, Co. Kilkenny, Summer 2018*. Included in Appendix 2 of the Ornithology chapter in the Castlebanny Wind Farm Environmental Impact Assessment Report.
- MWP (2019c). *Ornithology Report, Castlebanny, Mullinavat, Co. Kilkenny, Winter 2018/19*. Included in Appendix 2 of the Ornithology chapter in the Castlebanny Wind Farm Environmental Impact Assessment Report.
- MWP (2020). *Ornithology Report, Castlebanny, Mullinavat, Co. Kilkenny, Summer 2019*. Included in Appendix 2 of the Ornithology chapter in the Castlebanny Wind Farm Environmental Impact Assessment Report.
- SNH (2000). *Windfarms and Birds: Calculating a Theoretical Collision Risk Assuming No Avoiding Action*. Scottish Natural Heritage.
- SNH (2010). *Use of Avoidance Rates in the SNH Wind Farm Collision Risk Model*. Scottish Natural Heritage.
- SNH (2017). *Recommended Bird Survey Methods to Inform Impact Assessment of Onshore Wind Farms*. Scottish Natural Heritage.
- SNH (2018). *Avoidance Rates for the Onshore SNH Wind Farm Collision Risk Model*. Scottish Natural Heritage.
- Vessem, J. V. & Draulans, D. (1987). Patterns of arrival and departure of Grey Herons *Ardea cinerea* at two breeding colonies. *Ibis* 129, 353-363.

## Appendix 1 Parameter values used in the collision risk modelling

### INTRODUCTION

This appendix includes all the parameter values used in the collision risk modelling. The appendix first lists the general turbine parameters and bird species parameters, and then lists the specific parameters used in the basic and structured models. Rounded parameter values are shown for clarity, but the unrounded values were used in the models.

### GENERAL

Table A1.1. Wind turbine parameters used in the collision risk model.

Parameter	Value	Units	Details
$N_{\text{turbine}}$	21		Number of turbines
$H_{\text{hub}}$	107.5	m	Hub height
$H_{\text{rotor}}$	155	m	Rotor diameter
$H_{\text{rotor}(30-35)}$	5	m	Rotor length in the 30-35 m height band
$H_{\text{rotor}(35-135)}$	100	m	Rotor length in the 35-135 m height band
$H_{\text{rotor}(135-185)}$	50	m	Rotor length in the 135-185 m height band
$R_{\text{rotor}}$	77.5	m	Rotor radius
$A_{\text{rotor}(30-35)}$	184	m <sup>2</sup>	Rotor swept area in the 30-35 m height band
$A_{\text{rotor}(35-135)}$	13,422	m <sup>2</sup>	Rotor swept area in the 35-135 m height band
$A_{\text{rotor}(135-185)}$	5,263	m <sup>2</sup>	Rotor swept area in the 135-185 m height band
$b$	3		Number of blades in rotor
$C_{\text{max}}$	4.2	m	Maximum chord of rotor blade
$\gamma_1$	9°		Mean pitch angle of blade (data from a comparable onshore wind farm)
$\gamma_2$	27.5°		Mean pitch angle of blade (typical large turbine in an offshore wind farm)
OP	85%		Percentage of time the turbines will be operational

Sources:  $N_{\text{turbine}}$ ,  $H_{\text{hub}}$ ,  $H_{\text{rotor}}$ ,  $R_{\text{rotor}}$ ,  $b$ ,  $C_{\text{max}}$  and OP from specification provided;  $A_{\text{rotor}(25-35)}$ ,  $A_{\text{rotor}(35-50)}$  and  $A_{\text{rotor}(35-50)}$  calculated from  $H_{\text{rotor}}$  and  $R_{\text{rotor}}$  using Equation 5 and Equation 6 in Section 5.1.3;  $\gamma_1$  based on data from a comparable onshore wind farm (see Section 6.1);  $\gamma_2$  based on the typical range of mean pitch angles of 25-30° for modern turbines given by Band (2012).

Table A1.2. Bird species parameters used in the collision risk model.

Species	Speed (m/sec)	Body length (m)	Wingspan (m)	Avoidance rate
	$V_{bird}$	$L_{bird}$	$W_{bird}$	
Mallard	18.5	0.58	0.9	0.98
Cormorant	15.2	0.9	1.45	0.98
Grey Heron	12.5	0.94	1.85	0.98
Hen Harrier	9.1	0.6	1.44	0.99
Sparrowhawk	11.3	0.33	0.62	0.98
Buzzard	11.6	0.54	1.2	0.98
Golden Plover	17.9	0.71	1.58	0.98
Lapwing	12.8	0.3	0.84	0.98
Whimbrel	16.3	0.41	0.82	0.98
Curlew	16.3	0.55	0.9	0.98
Black-headed Gull	11.9	0.36	1.05	0.992
Lesser Black-backed Gull	13.4	0.58	1.42	0.995
Herring Gull	12.8	0.48	1.1	0.995
Kestrel	10.1	0.34	0.76	0.95
Peregrine	12.1	0.42	1.02	0.98
Mallard	18.5	0.58	0.9	0.98
Cormorant	15.2	0.9	1.45	0.98

$L_{bird}$  and  $W_{bird}$  values taken from [www.bto.org/about-birds/birdfacts](http://www.bto.org/about-birds/birdfacts).  $V_{bird}$  values taken from Alerstam et al. (2007); value for Grey Plover (*Pluvialis squatarola*) used for Golden Plover, as no value given for the latter species. Avoidance rates from SNH (2018) and Furness (2019).

## MODEL-SPECIFIC DATA

Table A1.3. Flight activity data (bird-secs) used in the combined VPs model for calculations of predicted transits.

Species	Height band		
	30-35 m	35-135 m	135-185 m
Mallard	36	375	0
Cormorant	0	60	0
Grey Heron	147	183	0
Hen Harrier	31	47	0
Sparrowhawk	232	1,009	107
Buzzard	1,834	9,440	1,519
Golden Plover	67	371	0
Lapwing	0	340	0
Whimbrel	158	51	0
Curlew	1,813	172	0
Black-headed Gull	2	87	78
Lesser Black-backed Gull (spring)	1,504	412	0
Lesser Black-backed Gull (breeding)	1,938	14,848	1,491
Lesser Black-backed Gull (autumn)	3,317	29,382	430
Lesser Black-backed Gull (winter)	31	46	0
Herring Gull	0	53	0
Kestrel	5,941	6,899	272
Peregrine	70	478	0

Table A1.4. Flight activity data (bird-secs) used in the VP averaging and turbine averaging models for calculations of predicted transits.

Species	Height band	VP1	VP2	VP3	VP4	VP5	VP6	VP7	VP9
Mallard	30-35 m	0	0	0	0	36	0	0	0
	35-135 m	0	0	0	0	375	0	0	0
	135-185 m	0	0	0	0	0	0	0	0
Cormorant	30-35 m	0	0	0	0	0	0	0	0
	35-135 m	0	0	0	0	0	60	0	0
	135-185 m	0	0	0	0	0	0	0	0
Grey Heron	30-35 m	0	0	0	0	147	0	0	0
	35-135 m	0	0	0	0	183	0	0	0
	135-185 m	0	0	0	0	0	0	0	0
Hen Harrier	30-35 m	12	0	0	0	98	0	0	0
	35-135 m	0	0	0	0	47	0	0	0
	135-185 m	0	0	0	0	0	0	0	0
Sparrowhawk	30-35 m	34	14	4	81	30	65	0	3
	35-135 m	150	60	18	352	132	284	0	13
	135-185 m	16	6	2	37	14	30	0	1
Buzzard	30-35 m	167	8	389	850	247	64	108	0
	35-135 m	860	44	2,004	4,374	1,273	327	558	0
	135-185 m	138	7	323	704	205	53	90	0
Golden Plover	30-35 m	0	0	0	0	234	0	0	0
	35-135 m	0	0	0	34	337	0	0	0
	135-185 m	0	0	0	0	0	0	0	0
Lapwing	30-35 m	0	0	0	0	0	0	0	0
	35-135 m	0	0	340	0	0	0	0	0
	135-185 m	0	0	0	0	0	0	0	0
Whimbrel	30-35 m	0	523	0	0	0	0	0	31
	35-135 m	51	0	0	0	0	0	0	0
	135-185 m	0	0	0	0	0	0	0	0
Curlew	30-35 m	0	0	6,345	0	0	0	0	0
	35-135 m	0	0	0	0	0	0	0	172
	135-185 m	0	0	0	0	0	0	0	0
Black-headed Gull	30-35 m	0	0	0	2	0	0	0	0
	35-135 m	0	0	0	87	0	0	0	0
	135-185 m	0	0	78	0	0	0	0	0
Lesser Black-backed Gull (spring)	30-35 m	0	0	0	0	43	0	1,460	0
	35-135 m	0	0	0	0	279	0	132	0
	135-185 m	0	0	0	0	0	0	0	0
Lesser Black-backed Gull (breeding)	30-35 m	0	0	880	509	139	0	410	0
	35-135 m	24	0	2,102	2,941	234	259	58	9,230
	135-185 m	0	0	345	1,147	0	0	0	0
Lesser Black-backed Gull (autumn)	30-35 m	0	0	140	771	1,870	0	374	162
	35-135 m	0	0	892	9,324	7,087	0	90	11,990
	135-185 m	0	0	0	0	430	0	0	0
Lesser Black-backed Gull (winter)	30-35 m	0	0	0	31	0	0	0	0
	35-135 m	0	0	29	17	0	0	0	0
	135-185 m	0	0	0	0	0	0	0	0

Species	Height band	VP1	VP2	VP3	VP4	VP5	VP6	VP7	VP9
Herring Gull	30-35 m	0	0	0	0	0	0	0	0
	35-135 m	0	0	53	0	0	0	0	0
	135-185 m	0	0	0	0	0	0	0	0
Kestrel	30-35 m	390	345	1,593	1,667	1,314	37	408	187
	35-135 m	453	401	1,850	1,936	1,526	43	473	217
	135-185 m	18	16	73	76	60	2	19	9
Peregrine	30-35 m	0	0	182	9	55	0	0	0
	35-135 m	0	0	0	284	194	0	0	0
	135-185 m	0	0	0	0	0	0	0	0

Table A1.5. Flight activity data (bird-secs) used in the Lesser Black-backed Gull Stage 1 model for calculations of predicted transits.

Season	Flight activity category	Height bands		
		30-35 m	35-135 m	135-185 m
spring	high	1,504	412	0
	low	0	0	0
breeding	high	1,906	14,512	1,491
	low	32	335	0
autumn	high	3,270	28,403	430
	low	47	979	0
winter	high	29	43	0
	low	1	3	0

Table A1.6. Seasonal periods and the  $D_{\text{season}}$  values used in the Stage 1 models for calculating predicted transits, and the species-specific rotation speeds used in the Stage 2 model for calculating collision probability.

Species	Seasonal period	$D_{\text{season}}$ (hours)	Rotation speed (m/sec)
Mallard	all year	4,484	9.04
Cormorant	all year	4,484	9.04
Grey Heron	all year	4,484	9.04
Hen Harrier	Sep-Mar	2,117	9.44
Sparrowhawk	all year	4,484	9.04
Buzzard	all year	4,484	9.04
Golden Plover	Oct-Apr	2,152	9.47
Lapwing	all year	4,484	9.04
Whimbrel	Apr-May, Jul-Oct	4,484	8.60
Curlew	all year	4,484	9.04
Black-headed Gull	all year	4,484	9.04
Lesser Black-backed Gull (spring)	Mar-Apr	783	8.64
Lesser Black-backed Gull (breeding)	May-Jul	1,494	8.24
Lesser Black-backed Gull (autumn)	Aug-Oct	1,169	9.04
Lesser Black-backed Gull (winter)	Jan-Feb, Nov-Dec	1,038	9.44
Herring Gull	all year	4,484	9.04
Kestrel	all year	4,484	9.04
Peregrine	all year	4,484	9.04
Mallard	all year	4,484	9.04

$D_{\text{season}}$  values were calculated for each month using the *Daylength* script from Masden (2015) which, in turn is based on Forsythe et al., (1995), using an input latitude of 51.819110. They were then summed for each species across the months included in the seasonal period of occurrence. Rotation speed was calculated from the relationship between windspeed and rotation speed from the turbine specifications, using the mean windspeed over the seasonal period of occurrence (see Section 6.1).

Table A1.7. Vantage point survey effort (hours) used in the combined VP, VP averaging and turbine averaging models for calculations of predicted transits.

Species	Combined VP model	VP averaging and turbine averaging models							
		VP1	VP2	VP3	VP4	VP5	VP6	VP7	VP9
Mallard	113	144	84	144	144	144	84	48	72
Cormorant	113	144	84	144	144	144	84	48	72
Grey Heron	113	144	84	144	144	144	84	48	72
Hen Harrier	58	78	54	72	72	72	54	12	36
Sparrowhawk	113	144	84	144	144	144	84	48	72
Buzzard	113	144	84	144	144	144	84	48	72
Golden Plover	60	78	48	78	84	78	42	12	36
Lapwing	113	144	84	144	144	144	84	48	72
Whimbrel	57	72	42	69	69	66	42	39	42
Curllew	113	144	84	144	144	144	84	48	72
Black-headed Gull	113	144	84	144	144	144	84	48	72
Lesser Black-backed Gull (spring)	18	24	12	24	30	24	6	6	12
Lesser Black-backed Gull (breeding)	32	36	18	42	36	45	24	21	18
Lesser Black-backed Gull (autumn)	27	36	24	30	30	27	24	21	24
Lesser Black-backed Gull (winter)	36	48	30	48	48	48	30	0	18
Herring Gull	113	144	84	144	144	144	84	48	72
Kestrel	113	144	84	144	144	144	84	48	72
Peregrine	113	144	84	144	144	144	84	48	72
Mallard	113	144	84	144	144	144	84	48	72

The vantage point survey effort for the combined VP model was standardised to adjust for uneven survey effort between vantage points (see Section 5.1.5).

Table A1.8. Vantage point survey effort (hours) used in the Lesser Black-backed Gull Stage 1 model for calculations of predicted transits.

Season	Flight activity category	Survey effort (hours)
spring	high	19
	low	17
breeding	high	34
	low	29
autumn	high	26
	low	29
winter	high	33
	low	39

The vantage point survey effort was standardised to adjust for uneven survey effort between vantage points (see Section 5.1.5).

Table A1.9. Viewshed areas and turbine numbers used in the combined VP, VP averaging and Lesser Black-backed Gull Stage 1 models for calculations of predicted transits.

Model	Vantage points / flight activity category	Viewshed area (ha)	Number of turbines in viewshed
Combined VPs	all	873	21
VP averaging turbine averaging	VP1	122	5
	VP2	97	1
	VP3	83	6
	VP4	116	4
	VP5	180	5
	VP6	89	3
	VP7	107	3
	VP9	79	1
	Lesser Black-backed Gull Stage 1 model	high	507
low		366	9

Table A1.10. Allocation of turbines to viewsheds for the purposes of the turbine averaging model.

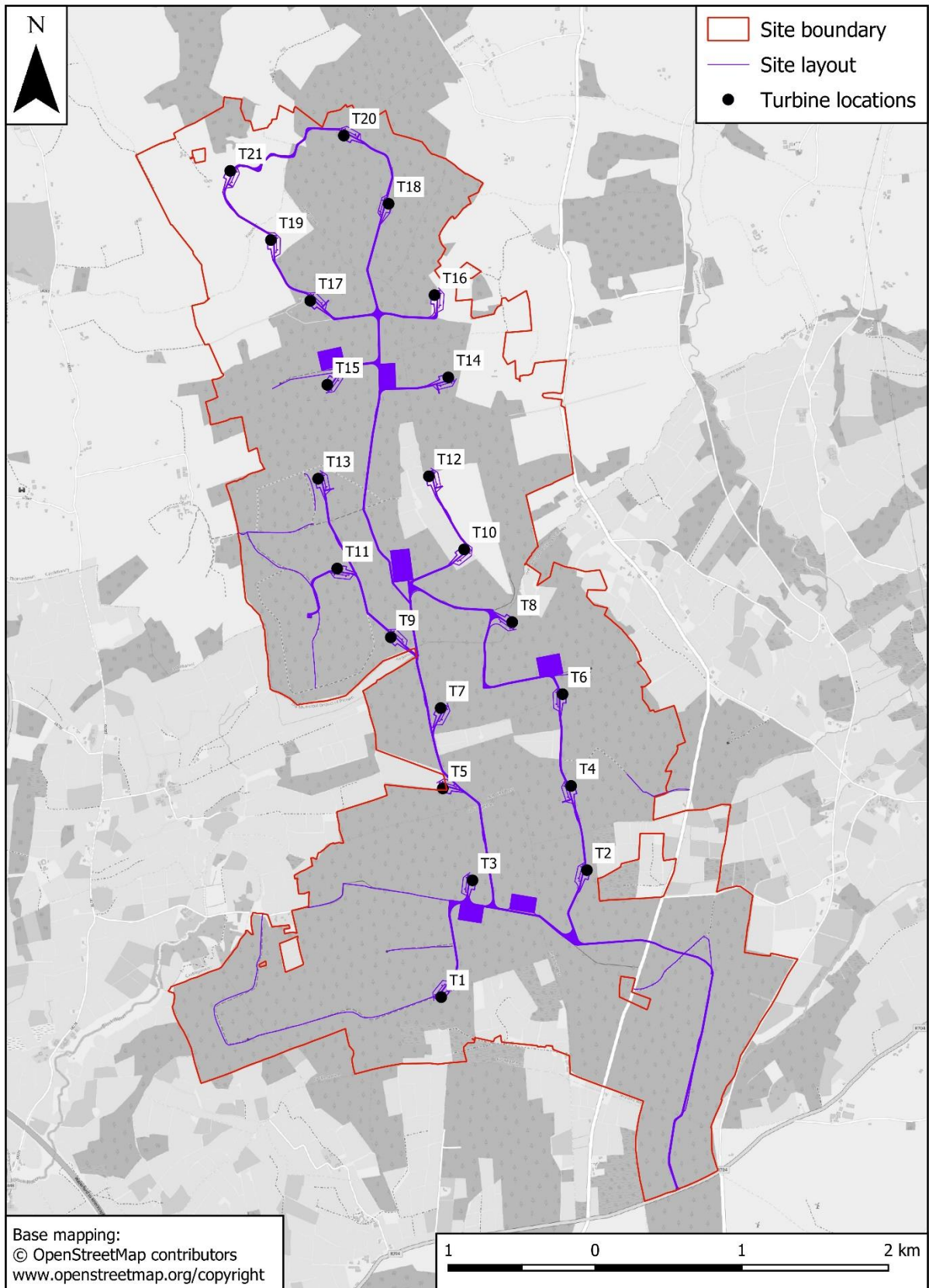
Turbine	Viewshed							
	VP1	VP2	VP3	VP4	VP5	VP6	VP7	VP9
T1								√
T2	√	√						
T3	√							
T4	√							
T5	√							
T6				√				
T7	√							
T8				√				
T9			√					
T10			√	√				
T11			√					
T12			√	√				
T13			√					
T14						√		
T15			√					√
T16						√		
T17					√			√
T18					√	√		
T19					√			√
T20					√			
T21					√			

## REFERENCES

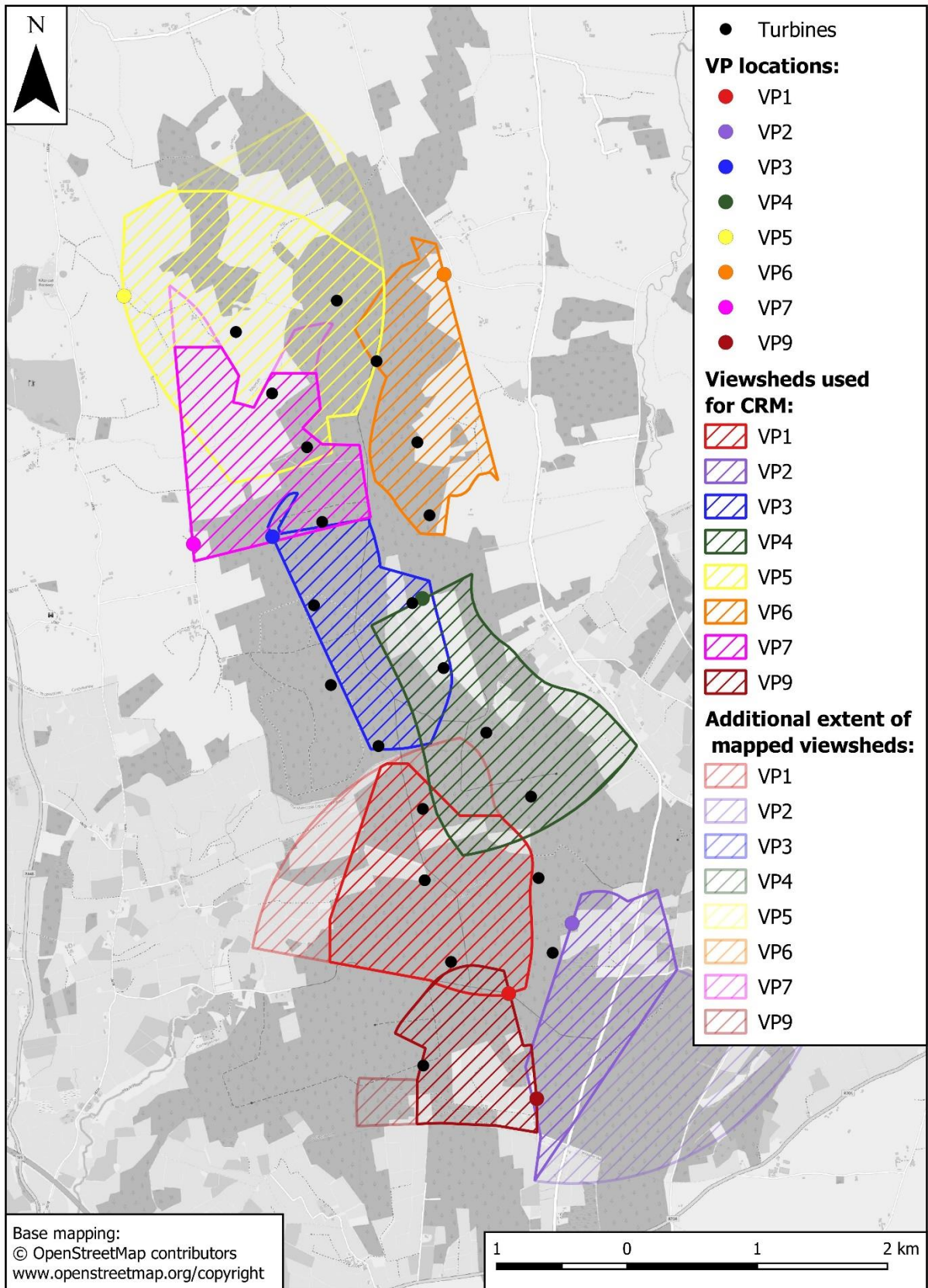
- Alerstam, T., Rosén, M., Bäckman, J., Ericson, P.G.P. & Hellgren, O. (2007). Flight speeds among bird species: allometric and phylogenetic effects. *PLoS Biol*, 5, e197.
- Forsythe, W. C., Rykiel Jr, E. J., Stahl, R. S., Wu, H. I., & Schoolfield, R. M. (1995). A model comparison for daylength as a function of latitude and day of year. *Ecological Modelling*, 80, 87-95.
- Furness, R.W. (2019). *Avoidance Rates of Herring Gull, Great Black-Backed Gull and Common Gull for Use in the Assessment of Terrestrial Wind Farms in Scotland*. Scottish Natural Heritage Research Report No. 1019. Scottish Natural Heritage.

Masden, E. (2015). *Developing an Avian Collision Risk Model to Incorporate Variability and Uncertainty*. *Scottish Marine and Freshwater Science Vol 6 No 14*. Scottish Government, Edinburgh.

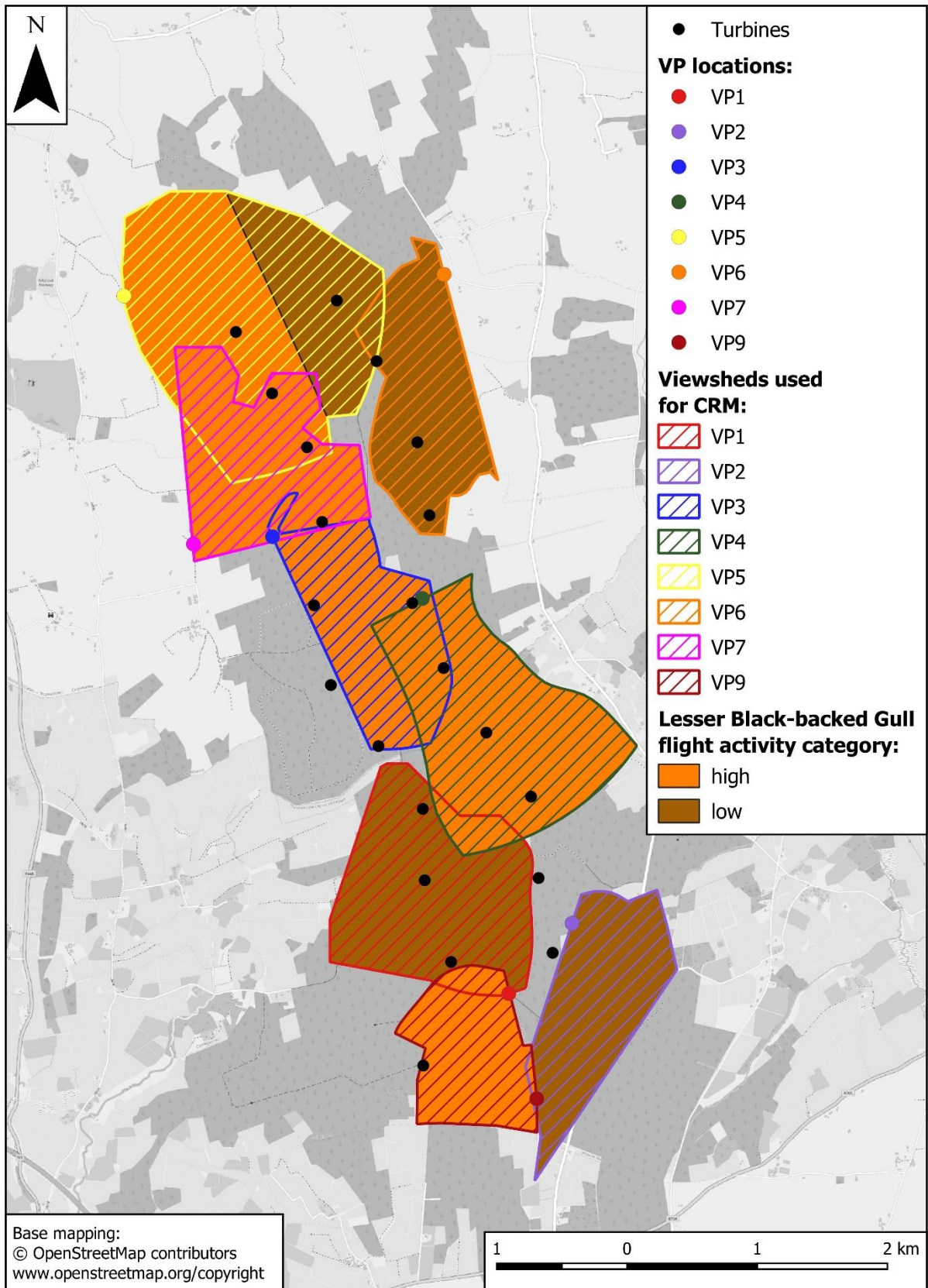
SNH (2018). *Avoidance Rates for the Onshore SNH Wind Farm Collision Risk Model*. Scottish Natural Heritage.



Map 1. Wind Farm site and layout.



Map 2. Vantage point locations and viewsheds included in the collision risk model.



Map 3. Lesser Black-backed Gull flight activity classification for the Lesser Black-backed Gull Stage 1 model.